Hydrogen reduction of lunar samples in a static system for a water production demonstration on the Moon

Planetary and Space Science 205 (2021) 105287

Contents lists available at ScienceDirect

Planetary and Space Science

journal homepage: www.elsevier.com/locate/pss

Hydrogen reduction of lunar samples in a static system for a water production demonstration on the Moon

H.M. Sargeant [a,*], S.J. Barber [a], M. Anand [a,b], F.A.J. Abernethy [a], S. Sheridan [a], I.P. Wright [a], A.D. Morse [a]

[a] School of Physical Sciences, The Open University, Walton Hall, Milton Keynes, UK
[b] The Natural History Museum, London, UK

ARTICLE INFO

Keywords:
Moon
Resources
Oxygen
Water
ISRU

ABSTRACT

In situ resource utilisation (ISRU) refers to the extraction and use of local materials, and numerous ISRU techniques have been proposed for use on the Moon. Hydrogen reduction of iron oxide-bearing minerals in the lunar regolith, such as ilmenite, has long been suggested as a potential method for producing water on the Moon to support exploration. Generally, reduction of lunar regolith has been proposed and tested in gas-flowing systems which utilise pumps to re-circulate gases (herein described as dynamic systems), and have been trialled in terrestrial laboratory and simulated environments. However, such technologies have yet to be validated on the lunar surface. An alternative to the dynamic reactor is a static system which utilises a cold finger to condense water from the vapour phase, negating the need for a more complex system where gases are continuously pumped away. The PROSPECT Sample Processing and Analysis (ProSPA) instrument is one such static system that is to be used to measure volatiles in the lunar regolith as a payload onboard the Luna-27 lander. Previous work using a breadboard model of ProSPA led to the development and optimisation of a procedure for extracting water from ilmenite. The present work describes the application of these procedures to the reduction of a lunar simulant (NU-LHT-2M), a lunar meteorite (NWA 12592), and two Apollo soils (10084 and 60500). Three 45 mg samples of each material type were reacted in a furnace at 1000 °C for 4 h in the presence of approximately 420 mbar of hydrogen. All samples reduced to some extent, with the Apollo mare soil (10084) producing the highest average yield of 0.94 wt % O_2; this compares favourably to the yields of ~3–4 wt % O_2 by other more optimised demonstrations of O_2 extraction from Apollo soils. Samples with higher ilmenite content produced higher yields, however, pyroxene and olivine within the samples also showed some minor reduction. The results demonstrate that a static system such as ProSPA is capable of reducing lunar regolith of various compositions and producing measurable yields of water. The technique is therefore appropriate for performing in situ resource utilisation experiments at the lunar surface. The simple and small scale technique is also appropriate for use in evaluating the grade of potential feedstock for the production of water by hydrogen reduction on the lunar surface.

1. Introduction

Water, and its constituents hydrogen and oxygen, are arguably the most imminently required resources on the lunar surface for long-duration missions on the Moon, and onward missions deeper into the solar system. Water and oxygen are critical for the life support needs of humans, while hydrogen and oxygen can be used for rocket propellant (Kornuta et al., 2019). Termed in situ resource utilisation (ISRU), extracting and making use of resources from the local environment, such as producing rocket propellant in situ on the Moon for return or onward journeys, will significantly reduce the initial launch mass from Earth.

1.1. An ISRU opportunity

The European Space Agency (ESA) ISRU roadmap comprises four steps as follows: “1) prospecting to characterize resource deposits; 2) technology verification and demonstration; 3) an ISRU pilot plant integrated with human missions; 4) full implementation" (Carpenter et al., 2016, 2018). The Package for Resource Observation and in Situ Prospecting for Exploration, Commercial exploitation and Transportation

* Corresponding author.
E-mail address: hannah.sargeant@open.ac.uk (H.M. Sargeant).

https://doi.org/10.1016/j.pss.2021.105287
Received 19 March 2021; Received in revised form 20 April 2021; Accepted 15 June 2021
Available online 18 June 2021

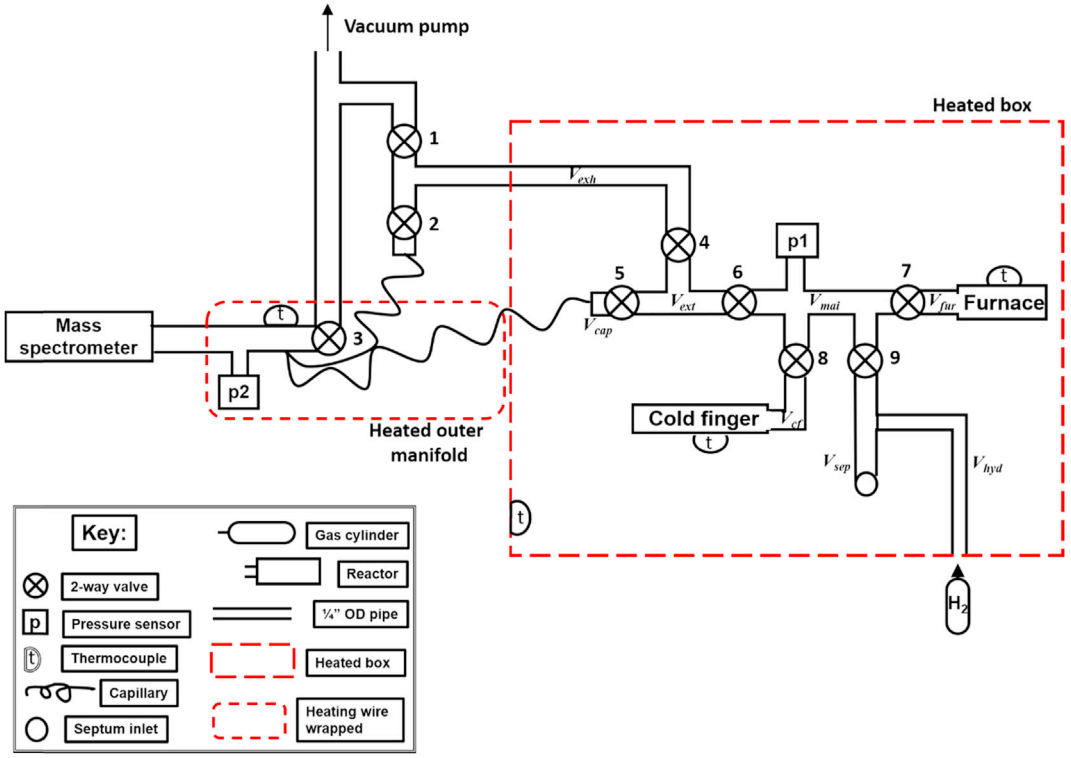

Fig. 1. A schematic of ISRU-BDM used in this study.

(PROSPECT) addresses the first two steps of the roadmap and is currently in development. The PROSPECT package will be flown on the Luna-27 lander, currently scheduled for launch in 2025, and consists of the PROSPECT Sample Excavation and Extraction Drill (ProSEED), and the PROSPECT Sample Processing and Analysis (ProSPA) suite (Sefton-Nash et al., 2018, 2020). Its aim is to extract samples, determine their volatile inventory, and assess resource potential of the Moon through ISRU experiments (Barber et al., 2018). ProSPA was not originally conceived with an ISRU focus, but previous work has assessed the opportunity that the package presents for performing an ISRU demonstration to produce water/oxygen from lunar regolith (Sargeant et al., 2020a). The ProSPA design contains a range of on-board gases (H_2, CO, CO_2, CH_4, N_2 and noble gases), a gas control system, pressure sensors, two cold fingers, two mass spectrometers, and a carousel of furnaces capable of heating samples up to 1000 °C. Of the multiple different techniques that could be used to extract oxygen from regolith (Schlüter and Cowley, 2020; Taylor & Carrier III, 1993), reduction by hydrogen was determined to be most suitable for implementation within ProSPA because it is feasible at temperatures of <1000 °C and because hydrogen is already available as part of the reference gas system.

1.2. Hydrogen reduction of regolith

The hydrogen reduction of regolith process is one of the most studied oxygen extraction processes for use on lunar materials, and has the highest Technology Readiness Level (TRL) of 5 indicating breadboard validation in a relevant environment (Sanders and Larson, 2012). The relative simplicity of the reduction process lends itself to the limited available hardware on ProSPA, however, the process results in the lowest potential yield of oxygen (in terms of water) as compared to other extraction processes because only iron oxides are reduced and the process is strongly influenced by ilmenite ($FeTiO_3$) content of the regolith (Schlüter and Cowley, 2020). Ilmenite comprises just a fraction of lunar soils which contain many other minerals of mostly basaltic and anorthositic origin (McKay et al., 1991a), however, ilmenite is the most easily reduced iron oxide-bearing mineral found in the lunar regolith (Allen et al., 1994).

Hydrogen reduction of regolith is an equilibrium reaction as shown in Eq. (1), where the reducing agent, H_2, loses electrons to the metal in the metal oxide, MO, within the regolith, and gains an oxygen.

$$MO + H_2 \leftrightarrow M + H_2O \quad (1)$$

Ilmenite reduction can be described more specifically in Eq. (2), where the hydrogen reduces the iron oxide, leaving a titanium dioxide product as well as the iron and water. At sufficiently high temperatures, TiO_2 (rutile) can be further reduced, but only after the ilmenite has been completely consumed (Zhao and Shadman, 1993).

$$FeTiO_3 + H_2 \leftrightarrow Fe + TiO_2 + H_2O \quad (2)$$

The equilibrium constant for the reaction is determined by the partial pressure of hydrogen and water (Sabat et al., 2014). In order to sustain the reduction process, the water vapour produced by the reaction must be constantly removed from the gas phase, e.g. flowing the gas mix to a condenser. Taylor et al. (1993) suggested that the ratio of H_2O vapour to H_2 at the reaction site must remain below 10% for the reaction to continue when operating at 1000 °C (gas pressures were not reported). Whereas work by Altenberg et al. (1993) suggests that in systems operating at 1000 °C with pressures of 1–100 mbar, the reaction would continue with >30% H_2O. Altenberg et al. (1993) also show that as the pressure increases beyond 1 bar, the permissible amount of water required for the reaction to continue reduces, which may explain the difference in values obtained by the two studies.

Iron oxides are the most easily reducible oxides (Lu et al., 2010; Sabat et al., 2014) and aside from ilmenite, evidence of reduction of iron oxide-bearing pyroxenes and olivines has also been demonstrated previously in fluidised (dynamic) systems (Britt, 1993; Massieon et al., 1992, 1993), including the reduction of Apollo soils (Allen et al., 1994, 1996, 1996; Gibson et al., 1994). Reduction reaction demonstrator concepts such as the Regolith and Environment Science, Oxygen and Lunar Volatiles Extraction (RESOLVE) payload, the Precursor ISRU Lunar Oxygen Testbed (PILOT) project, and the ROxygen project successfully reduced

iron oxide-bearing minerals in terrestrial field tests (Sanders and Larson, 2012). Each demonstration utilised a flow of hydrogen gas in dynamic reactor systems (Keller et al., 2009; Kleinhenz et al., 2009; Lee et al., 2013). In dynamic reactors there is a bulk flow of hydrogen gas over the regolith which carries the produced water away from the reaction site. Meanwhile static reactors are reliant on the diffusion of water molecules from higher concentrations at the reaction site through hydrogen gas to low concentrations of water vapour at a cold finger (where water condenses). Therefore, the rate of reaction will be slower in static reactors assuming the diffusion of water away from the reaction site is the rate controlling step. It is of interest to consider whether a ProSPA-like static system is able to demonstrate measurable reduction of lunar-like material which includes the reduction of other minerals as well as ilmenite.

A static system approach: ProSPA is primarily an analytical instrument for volatiles prospecting and its mass budget of 10 kg precludes the inclusion of fluidised/rotating ovens or a recirculating gas pump as within conventional reduction demonstrators. Instead, a different approach has been developed, utilising the available hardware to evaluate the regolith at the Luna-27 landing site as a feedstock for oxygen production by reduction with hydrogen. The iron oxide-bearing regolith is exposed to hydrogen (in a closed system), while a cold finger condenses any produced water (Williams, 1985), thus removing water from the reaction site and enabling the reaction to continue. This we term a 'static' process as distinct from the conventional dynamically pumped systems. A static system has not yet been used to reduce lunar simulants or samples. In this work we investigate whether a ProSPA-like system can demonstrate measurable reduction of lunar material which includes the reduction of other minerals as well as ilmenite.

A breadboard model comprising commercial off the shelf (COTS) versions of the relevant ProSPA hardware was developed at The Open University (Sargeant et al., 2020b). Termed the ISRU-BDM, it includes a furnace, a cold finger, a hydrogen supply, and a mass spectrometer (Fig. 1). The furnace, cold finger, and interconnecting manifold are contained within a heated box so that the pipework between the key components that may be exposed to water vapour is at a uniform temperature (within ±2.5 °C, the resolution of the thermocouples). The heated box is made from vermiculite sheets on a 100 × 65 × 75 cm aluminium frame and is heated to ~120 °C by two 2 kW oven heating elements. Swagelok® 4-VCR pipe and fittings are used throughout. High temperature (up to 315 °C) Swagelok® actuator valves (SS-4BG-V51-3C) with stainless steel spherical tips are used inside the heated box to control the movement of gases. A high temperature (temperature rated up to 120 °C) Kulite® diaphragm pressure sensor (ETL-641-375M-1.6BARA) is used to monitor the gas pressure in the system. The sensor has a sensitivity of 2.524 mV $mbar^{-1}$ which equates to a resolution of 0.06 mbar. When the heating elements are activated, the internal manifold heats uniformly to 114 ± 2.5 °C ensuring water contained within remains in the vapour phase up to pressures of 1.6 bar. The furnace utilises a ceramic chamber wrapped in resistance wires to heat samples up to 1100 °C. The ceramic (99.7% Al_2O_3 purity) sample tube is closed at one end and has dimensions of 200 mm length, 4 mm ID, and 6 mm OD. Before each experiment was performed a 45 mg sample was placed inside the sample tube which was then attached to the manifold within the heated box. The system is connected to an outer manifold, where the Hiden HPR-20 quadrupole mass spectrometer is located, via an exhaust pipe and capillary tubes. Of the outer manifold, all but the mass spectrometer are heated to 100 °C with Omega™ resistance heating wire. The vacuum pump is capable of achieving pressures of $<10^{-6}$ mbar inside the manifold. K-type thermocouples are used to record temperatures in the furnace, cold finger, heated box, and outer manifold. The ISRU-BDM valves and heaters are controlled by LabVIEW™ software enabling automated time-sequenced experiments.

A pathfinder study with the ISRU-BDM (Sargeant et al., 2020b) showed that 45 mg samples of 95% pure ilmenite grains could be reduced to produce yields of 3.51 ± 0.05 wt % O_2 (in terms of the water produced) over a reaction time of 4 h (the estimated time frame for ISRU experiments with ProSPA). The highest yield was obtained with an initial hydrogen pressure of ~420 mbar, and a furnace temperature of 1000 °C. Temperatures higher than 1000 °C resulted in higher yields but are beyond the capabilities of ProSPA, and therefore, not discussed in this paper.

Table 1
Chemical composition of NU-LHT-2M, NWA 12592, 10084, and 60500. The NU-LHT-2M and EATG treated NWA 12592 data were collected by IC-PMS measurements of three repeats, with uncertainty given as 1 SD. The 10084 and 60500 data are taken as the average of multiple analyses as compiled by Meyer (2009, 2010), with uncertainties given as 1 SD of all results. Values underlined are recalculations from the given iron oxide measurements and not included in totals.

Oxides	Concentration (wt %)			
	NU-LHT-2M	NWA 12592	10084	60500
Al_2O_3	23.62 ± 0.34	26.18 ± 0.38	13.67 ± 0.27	26.43 ± 0.64
CaO	13.33 ± 0.42	16.13 ± 0.66	12.1 ± 0.45	15.59 ± 0.28
Fe_2O_3	4.03 ± 0.5	4.37 ± 0.13	17.59 ± 0.52	6.24 ± 0.31
FeO	3.59 ± 0.44	3.89 ± 0.11	15.66 ± 0.47	5.56 ± 0.27
K_2O	0.08 ± 0.01	-	0.14 ± 0.02	0.12 ± 0.01
MgO	8.18 ± 0.22	6.52 ± 0.2	7.87 ± 0.15	6.15 ± 0.35
MnO	0.07 ± 0.01	0.06 ± 0.01	0.21 ± 0.01	0.07 ± 0.07
Na_2O	1.44 ± 0.01	0.3 ± 0.05	0.44 ± 0.04	0.44 ± 0.04
P_2O_5	0.07 ± 0.01	0.05 ± 0.01	0.14 ± 0.08	0.11 ± 0.03
SiO_2	48 ± 0.64	44.6 ± 0.96	42.48 ± 0.2	45.2 ± 0.2
TiO_2	0.37 ± 0.02	0.17 ± 0.01	7.66 ± 0.65	0.6 ± 0.02
Total	99.2	98.4	100.4	100.3

2. Materials

In this work, reduction experiments were performed on a lunar simulant and actual lunar samples. The samples selected include a highland lunar simulant, a lunar meteorite, and two Apollo lunar soils.

2.1. Lunar simulant

The lunar highland simulant NU-LHT-2M was selected because it provides a 'worst-case-scenario' for reduction with hydrogen. If the reduction reaction is feasible in highland-like materials, which are thought to have the lowest ilmenite contents, it should be feasible at all lunar locations. As well as using pure NU-LHT-2M, experiments were conducted on admixtures doped with increasing quantities of ilmenite to determine the effect on the yield of water, thus simulating the beneficiation of feedstock (Williams et al., 1979).

The simulant approximates the average bulk chemical composition of Apollo 16 regolith, and was created by Zybek Advanced Products Inc. using materials mostly sourced from Stillwater Mine in Nye, Montana (Manick et al., 2018). The simulant is designated 'M' (medium) as it has a grain size of <1 mm. A particular benefit of the Stillwater Mine material is that it contains high-calcium plagioclase which is abundant on the Moon yet rarely found in bulk on Earth (Rickman et al., 2014). The NU-LHT-2M simulant generally approximates lunar highlands soils in terms of the bulk mineralogy, presence of agglutinates, and grain size (Rickman and Lowers, 2012; Zeng et al., 2010). The main differences between NU-LHT-2M and lunar regolith are the geotechnical properties which are related to weathering processes (e.g. space weathering) on the Moon that are difficult to replicate on Earth. Consequently, like most simulants, NU-LHT-2M does not replicate the highly angular particle shapes found in lunar soils which affect cohesion and specific gravity (Zeng et al., 2010).

A bulk analysis of NU-LHT-2M was performed using inductively coupled plasma-mass spectrometry (ICP-MS) (Table 1). The bulk analysis shows that the maximum amount of ilmenite that could be present in the simulant is 0.7 wt % calculated stoichiometrically.

The NU-LHT-2M grains are mostly monomineralic (Rickman and Lowers, 2012), i.e. formed of one mineral. A small fraction of the grains

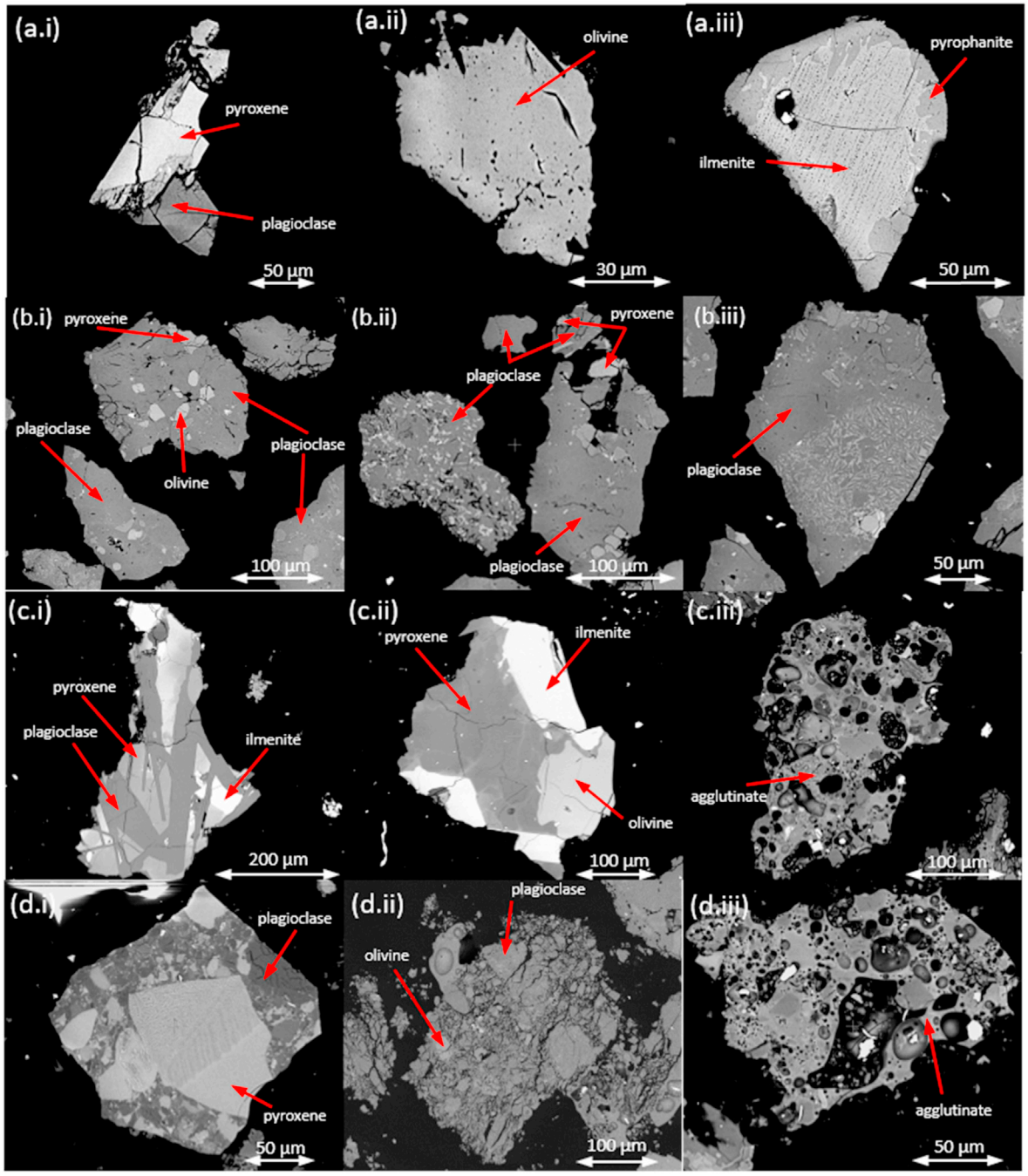

Fig. 2. BSE images of unreacted (a) NU-LHT-2M, (b) NWA 12592, (c) 10084, and (d) 60500. Untreated meteorite grains are shown in (b.i), while EATG treated meteorite grains are shown in (b.ii) and (b.iii).

include multi-phase minerals which can include combinations of plagioclase, pyroxene, and olivine. The simulant also contains synthetic agglutinates, made from partially and fully melted material (Zeng et al., 2010). The ilmenite grains in the simulant contain some pyrophanite ($MnTiO_3$), the manganiferous endmember of the ilmenite solid solution series which is less susceptible to reduction. Although there is only minor ilmenite content, NU-LHT-2M contains significant quantities of pyroxene and olivine totalling 15.7 vol % (Rickman and Lowers, 2012) which are other reducible FeO-bearing minerals (Massieon et al., 1992, 1993). Similarly, the glass present in the simulant also contains some iron oxides (Stoeser et al., 2010). Therefore, there are multiple components of the simulant that could be reduced in the presence of hydrogen to produce water, with ilmenite being the most easily reduced albeit present in low abundances. It should be noted that the nature of the iron found in lunar simulants can vary significantly from the iron found in lunar material. Iron oxides of terrestrial origin contain Fe^{2+} and Fe^{3+}. The more oxidised Fe^{3+} is found in Fe_2O_3 and therefore has more available oxygen than FeO which contains Fe^{2+}. The low oxygen fugacity of the lunar environment means that iron oxides are mostly Fe^{2+}. Therefore, there is less available oxygen in lunar iron oxides than terrestrial iron oxides (Taylor and Liu, 2010). The distribution of FeO and Fe_2O_3 in NU-LHT-2M is unknown, however, typical terrestrial rocks have a Fe^{2+}:Fe^{3+} ratio of 90:10.

2.2. Lunar meteorite

The lunar meteorite selected for analysis was North West Africa

(NWA) 12592, which has been classified as a fragmental regolith breccia (Meteoritical Bulletin Database, 2019). NWA 12592 was chosen because sufficient mass (~2 g) was available and the meteorite was deemed a suitable representative of a bulk lunar highlands regolith. The meteorite comprises lithic clasts which are dominated by pyroxene and plagioclase with minor olivine components, with the mineral clasts mainly comprising olivine, plagioclase, chromite, troilite, and Fe–Ni phases (Meteoritical Bulletin Database, 2019). Bulk-rock analysis of the meteorite was performed (Table 1). The analysed sample was crushed and had weathering products removed prior to ICP-MS analysis (see below). The TiO_2 content is very low at 0.17 ± 0.01 wt %, and there was no identifiable ilmenite present, (although stoichiometrically there is potential for 0.32 wt % ilmenite to be present, which is ~50% of that calculated for NU-LHT-2M). The iron oxide content is therefore attributed to the pyroxene and olivine. NWA 12592 has experienced moderate terrestrial weathering, a process leading to the formation of alteration products such as secondary carbonates and iron hydroxides on the surface of meteorites (Ali et al., 2016; Martins et al., 2007). If left untreated, these secondary iron oxides could also be reduced in the reduction experiments giving higher yields.

The powdering technique outlined in Mortimer (2016) was applied to a 2.12 g chip of NWA 12592, with the aim of approximating a lunar regolith-type consistency. Care was taken not to crush the meteorite into too fine a powder as any fine fractions would later be removed before experiments were performed to avoid damage to the ISRU-BDM. The final mass of the crushed NWA 12592 sample was 1.96 g with 0.16 g lost (a loss of 7.55%). The crushed meteorite contained a mixture of softer (anorthositic i.e. lighter material) and harder (basaltic i.e. darker) minerals, which made it difficult to produce a homogeneous grain size. As a consequence, the softer material would powder more quickly to a fine grain size and would remain in greater quantities as residue on the equipment during transfer, resulting in greater overall mass loss. It is therefore assumed that the majority of mass loss can be attributed to the loss of Fe-poor anothositic material, resulting in crushed meteorite samples with an increased iron content.

To limit the effects of weathering products on the final yield, half of the crushed meteorite samples were pre-treated with ethanolamine thioglycolate (EATG) to remove secondary oxides (Cornish and Doyle, 1984; Greenwood et al., 2012). The EATG treatment protocol is outlined in Appendix (A1). The EATG treatment had minimal effect on the mass of the crushed meteorite sample with just 2% mass loss as opposed to ~40–50% as often found using this technique (Personal Communication, R. Greenwood, November 19th, 2019). It was therefore assumed that there were minimal weathering products in the crushed sample (not treated by EATG) used for this study. Generally, meteorites contain a larger proportion of weathering products, and in such cases EATG treatment may be useful to ensure weathering products do not provide false-positive yields from the reduction of secondary oxides. The meteorite samples are herein denoted as untreated or treated.

2.3. Apollo soils

Two Apollo soils were selected for hydrogen reduction experiments. First an Apollo 11 mare soil, 10084, was selected as it is relatively rich in iron oxide-bearing minerals (Meyer, 2009). As a comparison, Apollo 16 highland soil, 60500, was selected for its relatively low iron oxide-bearing mineral content (Meyer, 2010). Together, the mare and highlands soils provide a range for the possible mineral composition expected on the lunar surface. Soil 10084 is the <1 mm sieve fraction of a contingency sample collected during Apollo 11. It was formed through impacts of meteorites on fine-grained basalt and breccia (Carrier III, 1973; Heiken, 1975), resulting in agglutinates, multi-phase grains and glassy particles. The mature soil mostly comprises glass, plagioclase, pyroxene, olivine and ilmenite. Based on the bulk TiO_2 content, the ilmenite present would be found in concentrations of up to 14.55 wt % (Table 1). The Apollo 11 soil should therefore be highly suitable for reduction with hydrogen to produce water.

In comparison, 60500 is a ≤1 cm sieve fraction of a rake sample collected during Apollo 16. Like 10084, the soil samples obtained during the Apollo 16 mission mostly comprise glassy agglutinates and multi-phase grains with plagioclase, pyroxenes, and olivine (The Lunar Sample Preliminary Science Team, 1972). The relatively low TiO_2 content (Table 1) indicates relatively low levels of potential ilmenite (up to 1.14 wt %) in the soil as compared to other lunar soil samples, and is expected to produce significantly lower yields than the 10084 soil.

2.4. Sample preparation

It is imperative that the grain size distribution of samples used in this work are representative of the expected grain size distribution of soils found on the lunar surface. The grain size influences reaction rate as it directly relates to the surface area of the reactant. However, there is a practical concern that the fine fractions may penetrate through the 2 μm filter and damage valves. Therefore, for this study the fines were removed. The simulant, meteorite, and Apollo soils were each sieved to remove the finer soil fractions (<38 μm). A smaller sieve mesh would be unsuitable for dry sieving (Retsch, 2004), while a larger sieve mesh would result in as much as 25% of the material being removed. Each sieved sample of ≥38 μm was used to prepare three 45 mg samples of each of the four material types for reaction.

2.4.1. NU-LHT-2M

The highlands simulant has a grain size distribution between 0.9 μm and 3 mm (Zeng et al., 2010). A single sample of 2.113 g of NU-LHT-2M was sieved to remove fines. Scanning electron microscope (SEM) analysis of unreacted NU-LHT-2M grains was performed and example backscatter electron (BSE) images are shown in Fig. 2. Energy dispersive spectroscopy (EDS) was used to identify the minerals present.

Sieved simulant was also used to prepare ilmenite-doped samples using 95% pure ilmenite powder with an average grain size of ~170 μm which was used in previous work (Sargeant et al., 2020a, 2020b). The ilmenite feedstock was supplied by A. Cowley from the European Astronaut Centre (EAC), who sourced the material from the Mineral Trade Company (GmD Mineral Trade Company, 2020). The samples were combined in different ratios of NU-LHT-2M to $FeTiO_3$ (100:0, 90:10, 75:25, 50:50, and 25:75). Mixtures of up to 75% ilmenite were analysed to represent a range of beneficiation grades (Williams et al., 1979).

2.4.2. NWA 12592

Each of the three untreated and treated meteorite samples were sieved separately to evaluate any heterogeneity within the samples. The grain size of the sieved meteorite samples was measured using a Nikon SMZ1500 microscope and images taken with infinity capture software at a magnification of 10 × before being analysed in Image J open source software. Assuming that the grains are spherical, the grain diameters were determined to be between 28 and 429 μm with an average diameter of 70 μm across the randomly selected grains analysed (n = 295). Each sieved sample of ≥38 μm was used to prepare a 45 mg sample for reaction. SEM images show how most grains produced from the crushing of the meteorite resulted in mostly composite grains, with some monomineralic grains (Fig. 2). There was no noticeable difference in the appearance of grains between the untreated and treated samples, suggesting there are minimal weathering products present in the crushed meteorite. EDS analysis with the SEM identified most composite grains as containing olivine and pyroxene inclusions set within a fine-grained regolith matrix.

2.4.3. 10084 & 60500

The Apollo soils each contain a high proportion of fines (Graf, 1993) that must be removed before use in the ISRU-BDM. Apollo soils are known to be electrostatic (Carrier III et al., 1991), and so an additional

Table 2
Operational conditions of the ISRU-BDM during each experimental stage.

Experimental stage	System conditions		
	Operational volume (10^{-6} m^3)	Cold finger temperature (°C)	Furnace temperature (°C)
Bake-out	47.3 ± 0.2	−80	500
H_2 addition	11.9 ± 0.2	−80	500
Reduction reaction	21.9 ± 0.1	−80	1000
Water release	21.9 ± 0.1	120	500

measure was applied to the protocol where a grounding cable was attached to the sieve to minimize any build-up of charge and additional sticking of the soil to the sieve. The ≥38 μm fractions were then used to prepare the 45 mg samples which were to be used in the reduction experiments. Example grains from each soil sample were imaged with the SEM and are shown in Fig. 2. The imaged grains are representative of the bulk sample which mostly contain multiphase grains and agglutinates. EDS analysis identified significant quantities of ilmenite and olivine with plagioclase and pyroxene in the multiphase grains in the 10084 soil. Meanwhile, olivine was scarce and ilmenite was not identified in the selection of imaged 60500 grains.

3. Methodology

Each material (simulant, meteorite, and lunar soils) was prepared, reacted, and analysed in triplicate. Each prepared sample, with a mass of 45 ± 0.5 mg, was placed into a ceramic sample holder which was attached to the ISRU-BDM manifold and held at an initial pressure of

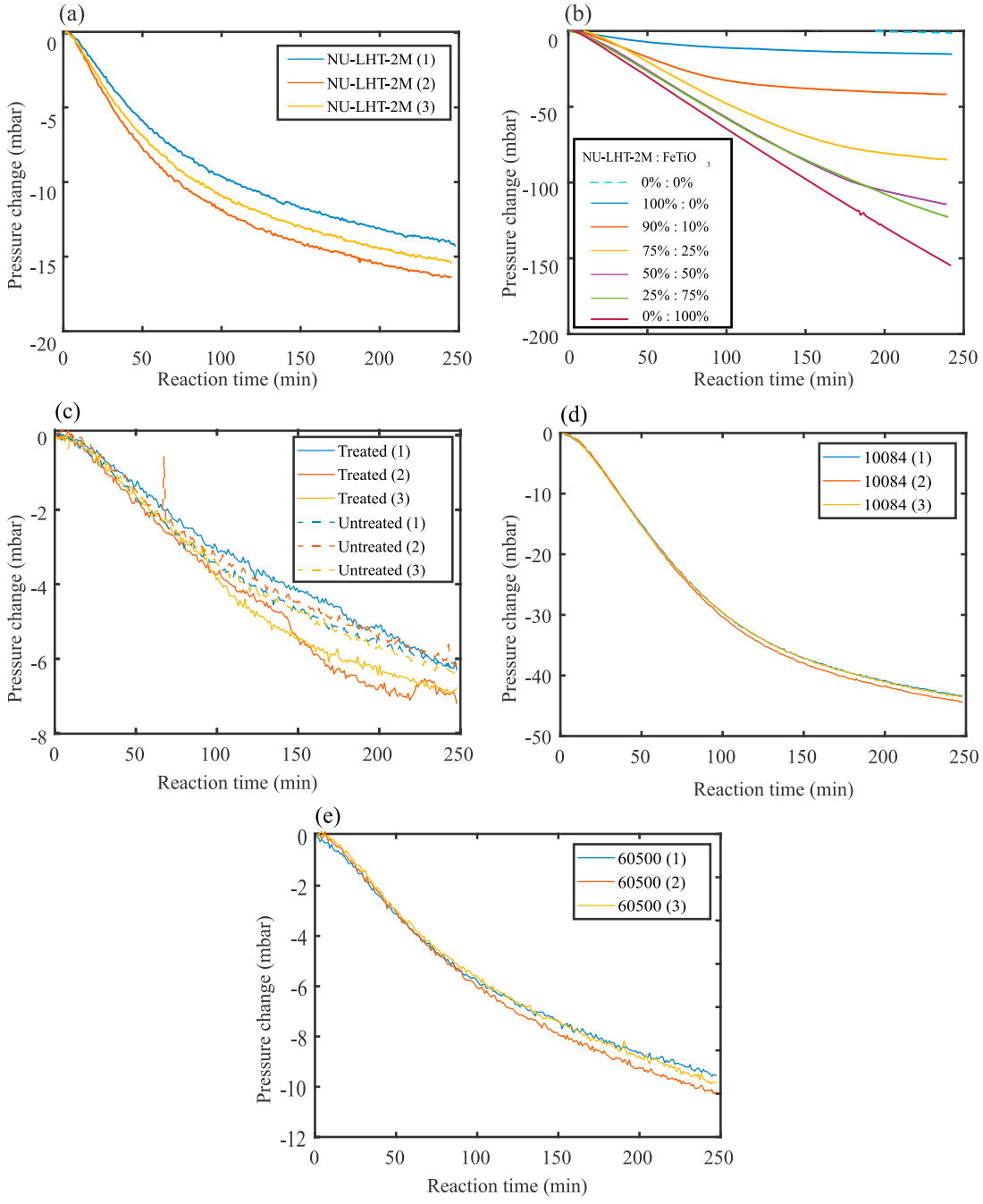

Fig. 3. Pressure change during the hydrogen reduction of (a) NU-LHT-2M, (b) ilmenite-doped NU-LHT-2M, (c) NWA 12592, (d) 10084, and (e) 60500.

Table 3
Results from the reduction reaction phase. Ilmenite results are obtained from raw data in Sargeant et al. (2020) and processed in the same way as results obtained in this work.

Sample	P_{H2i} (mbar)	ΔP_{cr} (mbar)	n_h (μmol)
NU-LHT-2M	436 ± 11	−14.5 ± 1.1	9.7 ± 0.7
90%:10% (NU-LHT-2M:ilmenite)	428.6 ± 0.5	−41.4 ± 0.5	27.7 ± 0.5
75%:25% (NU-LHT-2M:ilmenite)	460.4 ± 0.5	−84.4 ± 0.5	56.5 ± 0.9
50%:50% (NU-LHT-2M:ilmenite)	424.4 ± 0.5	−114.5 ± 1.1	76.7 ± 1.2
25%:75% (NU-LHT-2M:ilmenite)	431.0 ± 0.5	−123.2 ± 0.5	82.9 ± 1.2
Ilmenite	418.4 ± 0.5	−156.0 ± 0.5	104.5 ± 0.8
NWA 12592 (untreated)	439 ± 23	−5.3 ± 0.2	3.5 ± 0.1
NWA 12592 (treated)	424.0 ± 0.9	−5.8 ± 0.5	3.9 ± 0.3
10084	426.9 ± 5.7	−43.1 ± 0.5	28.9 ± 0.3
60500	424.1 ± 0.5	−8.9 ± 0.4	6.0 ± 0.2

$<10^{-5}$ mbar. They were baked for 2 h at 800 °C to account for any terrestrial hydration or mineral decomposition and the evolved gases were removed via the vacuum pump. Mass spectrometer readings were recorded during the bake-out of each sample and can be seen in Appendix A2. Most volatiles were removed from the samples within the first 30 min, with water (m/z 18) the slowest to be removed from the sample/vacuum system. The vacuum pump recorded a pressure reading of $\leq 10^{-6}$ mbar after 2 h, which was deemed sufficient for starting the ilmenite reduction experiments as it is significantly below the uncertainty in pressure readings in the ISRU-BDM (±0.5 mbar).

The same experimental procedure was followed as in Sargeant et al. (2020b), and applying the optimum reaction conditions determined therein (Table 2). First, ~0.3 mmol of H_2 (a target of ~420 mbar) was inserted into the operational volume where it reacted with the sample at 1000 °C. During the reaction any water produced diffused to the cold finger which was maintained at −80 °C and condensed. After 4 h the remaining gases were evacuated from the system before the system was sealed under vacuum and the cold finger was heated to 120 °C. The released water was then recondensed at the cold finger before a final release so that the volatiles could be analysed by the mass spectrometer.

4. Results

4.1. Reaction phase

During the reaction the gas pressure drops as hydrogen is consumed and the resultant water is condensed at the cold finger. The pressure change during the reaction for each material type is shown in Fig. 3. Three samples of each material were reacted, except for the doped simulant, for which only one experiment was performed for each respective ratio of simulant to ilmenite. The results are summarised in Table 3, where the initial hydrogen pressure, P_{H2i}, the total corrected pressure change, ΔP_{cr}, and the amount of hydrogen used in the reaction, n_h, are shown. Where repeat measurements were taken the average result and 1 SD is provided; for the complete results see Appendix A3. Uncertainty in individual pressure readings is expressed as the variability of pressure readings as determined when air was held in the manifold for 1 h (±0.5 mbar). The total corrected pressure change during the reaction phase is calculated by first subtracting the associated blank reading (6.1 mbar), obtained when an empty sample tube was reacted under the same conditions. The pressure values are then calibrated to be representative of a uniform 120 °C system by multiplying by the temperature calibration factor (1.048) obtained from Sargeant et al. (2020b). The corrected pressure change is then used to estimate the quantity of hydrogen used in the reaction using the ideal gas equation: $n = PV/RT$, where V is the system volume (Table 2), R is the ideal gas constant, and T is 120 °C (393 K).

Table 4
Results from the water release phase. Ilmenite results are obtained from raw data in Sargeant et al. (2020) and processed in the same way as results obtained in this work.

Sample	ΔP_{cw} (mbar)	n_w (μmol)	O_2 yield (wt % O_2)
NU-LHT-2M	12.0 ± 1.5	8.0 ± 0.1	0.28 ± 0.04
90%:10% (NU-LHT-2M:ilmenite)	37.2 ± 0.5	24.9 ± 0.5	0.89 ± 0.02
75%:25% (NU-LHT-2M:ilmenite)	79.5 ± 0.5	53.2 ± 0.6	1.89 ± 0.03
50%:50% (NU-LHT-2M:ilmenite)	106.2 ± 0.5	71.1 ± 0.7	2.50 ± 0.04
25%:75% (NU-LHT-2M:ilmenite)	115.7 ± 0.5	77.5 ± 0.8	2.75 ± 0.04
Ilmenite	147.4 ± 0.5	98.7 ± 1.0	3.51 ± 0.05
NWA 12592 (untreated)	3.4 ± 0.3	2.3 ± 0.3	0.08 ± 0.01
NWA 12592 (treated)	2.8 ± 0.7	1.8 ± 0.3	0.07 ± 0.02
10084	39.3 ± 1.3	26.3 ± 0.9	0.94 ± 0.03
60500	7.6 ± 0.8	5.1 ± 0.5	0.18 ± 0.02

4.2. Water release phase

After the reaction phase, the cold finger is heated and the condensed water released as a vapour. The associated pressure change in the system, ΔP_{cw}, is recorded in Table 4, along with the calculated amount of water released, n_w, and the equivalent yield in terms of wt % O_2 (Hadler et al., 2019). The associated pressure change during the water release phase is corrected by subtracting the corresponding blank value (5.2 mbar for the water release phase). The blank value was obtained by recording the pressure change when an empty sample tube was reacted under the same conditions. Subtracting this value from those obtained from reacted samples ensures that the calculated yields are a result of the reduction of the samples only. The amount of water produced is calculated using the ideal gas equation as for n_h. The yield is calculated using Eq. (3), where M_o is the molar mass of oxygen, and m is the mass of sample. The uncertainty in water production rate, total water produced, and oxygen yield, was calculated from the propagation of uncertainties in the measured pressure, operational volume, and manifold temperature values (±0.5 mbar, $\pm 1.49 \times 10^{-7}$ m^3, and ±2.5 °C respectively). The uncertainty in average values was calculated as a 1 SD uncertainty in the three repeats.

$$wt\ \%\ O_2 = \frac{n_w M_o}{m} \quad (3)$$

4.3. Reacted sample analysis

SEM analyses were performed on each material type (Fig. 4). BSE imaging and EDS analysis of polished reacted grains were used to identify the presence of the reaction product iron, and identify in which minerals the reaction had occurred. The bright white streaks and blebs in BSE images are indicative of iron deposits, and show that ilmenite grains generally react to completion, while olivine, pyroxene, and even some plagioclase, show partial reduction.

5. Discussion

The results show that each sample reduced to some extent, with the doped simulant and 10084 soil producing the highest yields (excluding the results obtained in (Sargeant et al. (2020b) with pure ilmenite). The meteorite samples produced the lowest yields, followed by the iron oxide poor 60500 lunar soil. It would be reasonable to assume that the untreated meteorite samples would have more iron oxides present from weathering products and therefore produce higher yields than the treated samples. The untreated samples did result in slightly higher (3.4 ± 0.3 mbar) calculated yields compared to the treated sample (2.8 ± 0.7 mbar) in the water release phase, but not in the reaction phase (5.3 ± 0.2 mbar to 5.8 ± 0.5 mbar respectively). It should also be noted that the resultant yields for the untreated and treated samples are within error of each

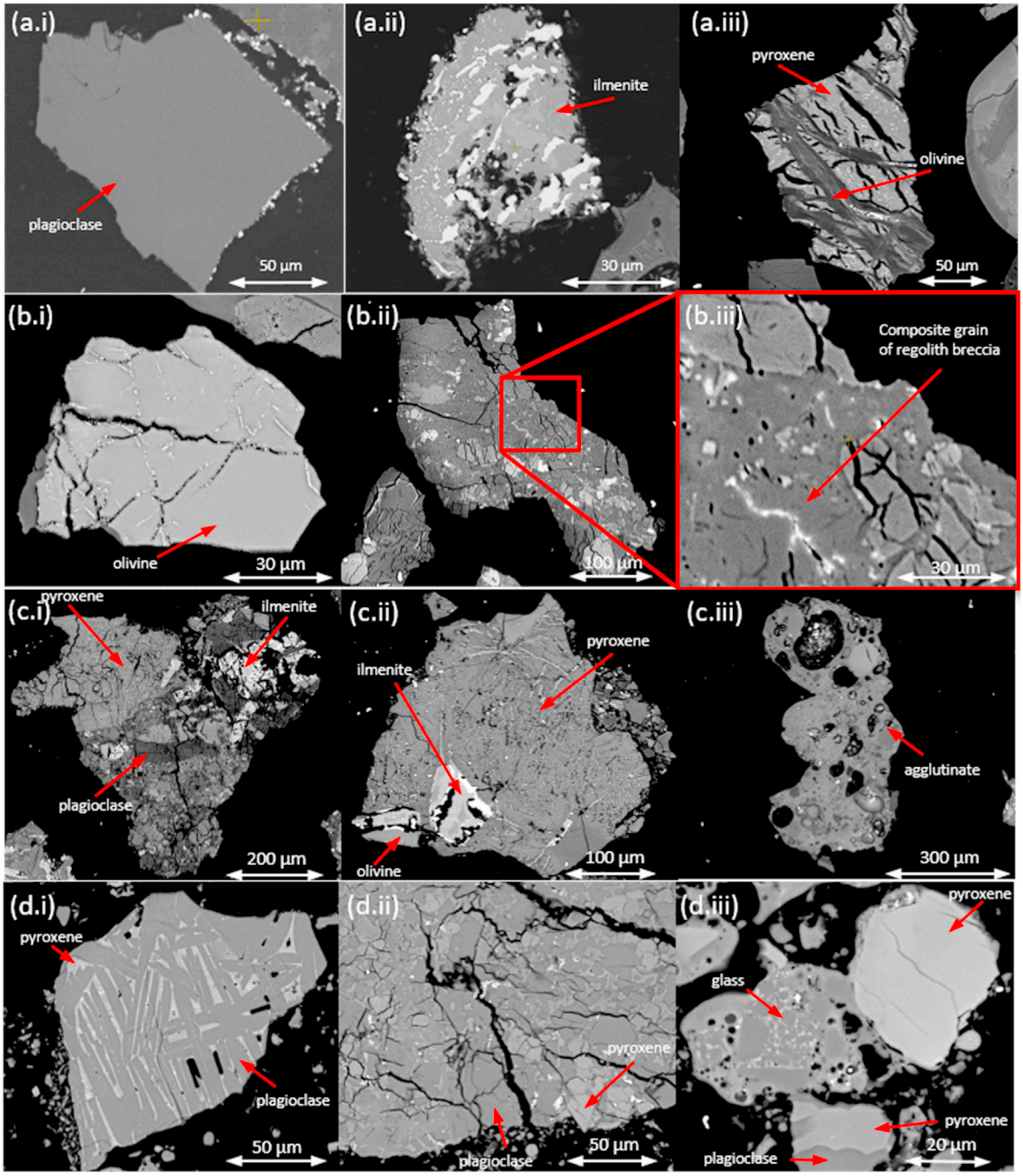

Fig. 4. BSE images of reacted (a) NU-LHT-2M, (b) NWA 12592, (c) 10084, and (d) 60500.

other. Considering also that the EATG treatment only resulted in a mass loss of 2% it is concluded that the EATG treatment had a negligible effect on the reaction, indicating that there were little if any weathering products present in the samples that were reacted.

5.1. Water losses

With more ilmenite present in a sample, there was a greater discrepancy in the amount of hydrogen used and the amount of water produced (n_h-n_w). It is believed that residual water was trapped within the grains when the reaction was halted before completion. If there is a larger amount of reducible material within the sample, then there will be more water molecules retained when the reaction is terminated (Fig. 5).

A plot of n_h-n_w against yield for all samples reacted in the ISRU-BDM is shown in Fig. 6. It can be seen that there is a clear correlation, with higher yields recorded when n_h-n_w is higher. Some water will always adsorb onto the stainless steel manifold, hence there will always be a non-zero value for n_h-n_w, even for samples which are assumed to have reacted to completion (or near completion) including the meteorite samples and the Apollo 16 soil.

5.2. Estimating yields

The results of hydrogen reduction of samples used in this work and of other materials reacted at 1000 °C are shown in Fig. 7 (Allen et al., 1994; Gibson et al., 1994; McKay et al., 1991b; Sueyoshi et al., 2008). It should

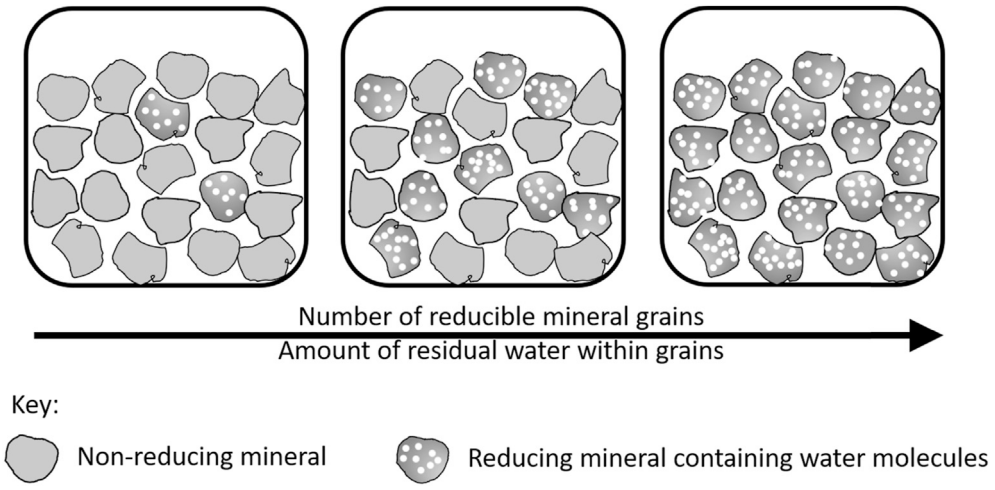

Fig. 5. A cartoon showing samples with increasing reducible mineral content. When the reaction is halted before completion, the samples with more reducible minerals contain more water molecules within the grains.

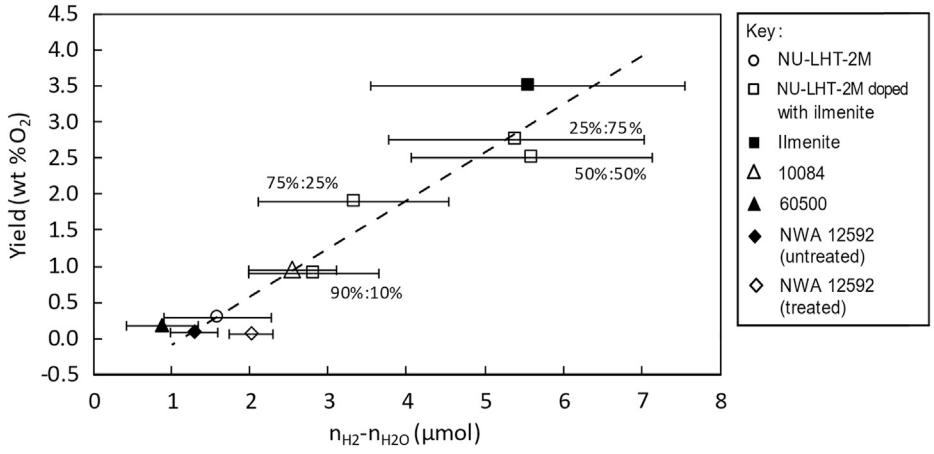

Fig. 6. Plot showing the discrepancy between the amount of hydrogen used in the reaction and the amount of water released from the cold finger (n_h-n_w) against the calculated yields. Results are shown for all samples reacted in the ISRU-BDM under the same conditions (1000 °C for 4 h with 0.3 mmol of hydrogen).

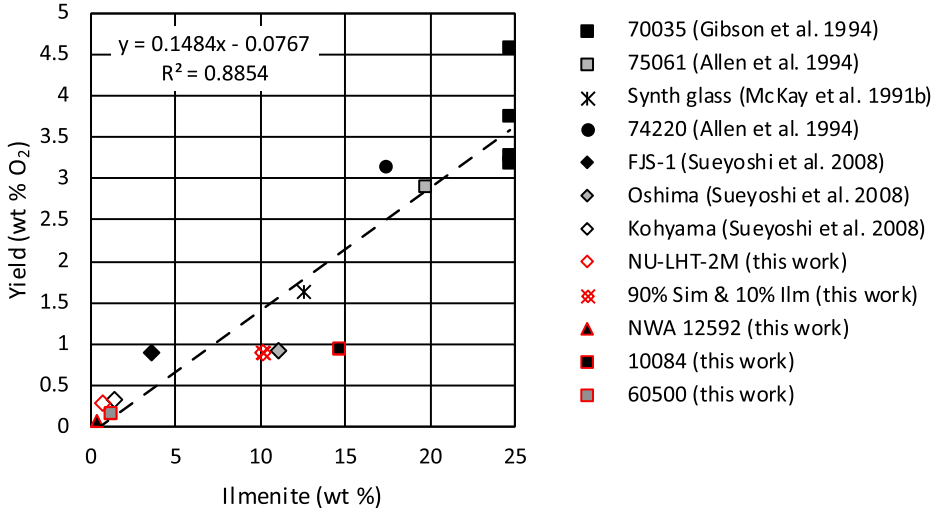

Fig. 7. Experimental yields from lunar soils and simulants reduced by hydrogen at 1000 °C and reacted to completion. Squares represent lunar soils, crosses represent synthetic glass, circles represent volcanic glasses, diamonds represent simulants, and triangles represent meteorites. Results are shown with respect to maximum possible ilmenite content.

be noted that the results from literature were obtained from fluidised systems with various hydrogen pressures, and that all of the samples were reacted to completion. It can be seen that ilmenite concentration strongly dictates yield of oxygen, with a non-zero yet relatively small yield produced by samples with no ilmenite but with other iron-oxide bearing minerals present. Higher than expected yields can be caused by reduction of the product rutile as seen in Gibson et al. (1994). Meanwhile, lower than expected yields are likely a result of either incomplete reaction and/or overestimated ilmenite contents.

The ilmenite contents plotted refer to stoichiometrically calculated values. Assuming all the TiO_2 present in each sample is found in ilmenite, a maximum possible ilmenite concentration is calculated (it should be noted that pyroxene does also have significant TiO_2 contents). The ilmenite estimations based on TiO_2 are upper limits and are more accurate in immature soils and terrestrial simulants as ilmenite is converted to impact glasses in mature soils, lowering the ilmenite content, while preserving the bulk TiO_2 content (Chambers et al., 1995). The two Apollo soils studied in this work are mature soils and therefore the ilmenite estimations are likely to be higher than the true values.

Other techniques can be used to estimate ilmenite content, including grain counting and X-ray digital imaging. Chambers et al. (1995) showed how these techniques can give vastly different contents. For example, the ilmenite content in Apollo soil 10084 can be calculated as 4.2 wt %, 10.2 wt %, and 14.3 wt % when using grain counting, X-ray digital imaging, and stoichiometry respectively. It is thought that the commonly used grain counting technique will often underestimate the ilmenite content because it omits ilmenite that is found in multiphase grains that are commonly found in Apollo soils. When using X-ray digital imaging to determine the ilmenite content of the Apollo 11 sample, the ilmenite content of 10084 more closely resembles the ilmenite content of the doped simulant (90% NU-LHT-2M: 10% ilmenite) as 10.2 wt % and 10.1 wt % respectively. Both the Apollo sample and doped simulant also have similar yields (0.94 ± 0.03 wt % and 0.89 ± 0.02 wt % O_2 respectively) suggesting that accurately determined ilmenite content can be used to infer yields, and vice versa. It is postulated that when applying a consistent operating procedure, samples of lunar simulant and/or lunar soil could be reacted with a ProSPA flight model to produce a similar plot of ilmenite content vs yield. The resulting trendline could be used to infer ilmenite content of lunar soil at the Luna-27 landing site.

The high-latitude regions of the Moon where the Luna-27 mission is targeted to land (King et al., 2020) are known to have relatively low iron abundances (Lawrence et al., 2002; Spudis et al., 2013) indicating they comprise highland-type regolith and may be expected to contain low ilmenite contents. Ilmenite contents in lunar highland soils have been recorded as low as <1 wt % (Simon et al., 1982). In order for the experiments outlined in this work to be successful in producing and measuring water yields with the ProSPA instrument, the resultant pressures must exceed 0.25 mbar which is the minimum required resolution of ProSPA pressure sensors. When reducing a lunar soil sample with relatively low ilmenite content (60500) the pressure change recorded with the ISRU-BDM was 7.6 ± 0.8 mbar. It is expected that ProSPA will have a smaller volume than the ISRU-BDM, and therefore the equivalent pressures in the system would be even higher than those recorded in the ISRU-BDM. It is therefore expected that ProSPA could be used to produce measurable yields of water from samples at any landing site location.

5.3. Implications

The technique outlined in this work could be used on lunar soils obtained at various localities on the lunar surface as a proof-of-concept of water production from regolith. The experiments could follow on from evolved gas analysis experiments (Verchovsky et al., 2020) that are also planned to be performed with ProSPA, which would be equivalent to a bake-out of the samples. However, if considering a design to produce water in useable quantities to support a lunar base then adaptations would be required. For example, a fluidised bed would be recommended to improve the reaction rate (Hegde et al., 2011). Also, other products such as hydrogen sulfide would be produced in larger quantities from the reduction of sulfur-bearing minerals present in lunar samples. Such products could prove damaging to the system, and purification of the produced water would be required before it could be used (Sanders and Larson, 2012). Other techniques are likely more suitable to produce the large scale quantities of oxygen from lunar rocks and soils that are needed to support lunar bases, such as those that can reduce all oxides through electrolysis (Lomax et al., 2020). However, these techniques are more energy intensive and require substantial infrastructure. In comparison, the technique outlined in this work is relatively simple and can be applied with small instruments on the lunar surface in the very near future. Such an instrument could be used as a prospecting tool to measure the reducibility of regolith as well as performing other experiments such as evolved gas analyses to determine volatile inventory at multiple locations across the lunar surface. The results obtained from these in situ analyses could inform the development of larger scale reactors to produce sufficient supplies to support a lunar base.

6. Conclusion

Lunar soil simulants, lunar meteorites, and Apollo soils that contain iron oxide-bearing minerals can be reduced in a static system to produce water. Although ilmenite abundance strongly influences the yield, other minerals such as pyroxene and olivine will also reduce to some extent but make only minor contributions to yields. The highest yields were obtained for the mare Apollo soil (10084), producing on average 0.94 wt % O_2. Meanwhile, lower yields were obtained for the highlands Apollo soil (60500) producing an average of 0.18 wt % O_2. The technique outlined in this work is therefore recommended for use on small scale prospecting instruments as a proof-of-concept for early water production experiments on the Moon. The strong correlation between ilmenite content and yield means that a ProSPA-like instrument could be used to estimate the amount of reducible material in the lunar regolith, informing the location and requirements of future large scale reduction reactors.

CRediT authorship contribution statement

H.M. Sargeant: Conceptualization, Methodology, Investigation, Writing – original draft, revision. **S.J. Barber:** Supervising, Conceptualization, Methodology, Investigation, Writing – review & editing. **M. Anand:** Supervising, Investigation, Writing – review & editing. **F.A.J. Abernethy:** Supervising, Methodology, Investigation, Writing – review & editing. **S. Sheridan:** Supervising, Methodology. **I.P. Wright:** Supervising, Conceptualization, All authors approved and read the manuscript. **A.D. Morse:** Supervising, Conceptualization, Methodology, Investigation, Writing – review & editing.

Declaration of competing interest

The authors declare that they have no known competing financial interests or personal relationships that could have appeared to influence the work reported in this paper.

Acknowledgements

The funding by the Science and Technology Facilities Council (STFC) of a studentship for H.S. is acknowledged (#ST/N50421X/1). ProSPA is a programme of and funded by the European Space Agency (ESA). The research was partially supported by STFC grants to M. A. (#ST/P000657/1 & #ST/T000228/1). The EATG treatment on the meteorite samples was carried out by J. Gibson and J. Malley at The Open University. ICP-MS bulk analyses of the samples were performed by E. Humphreys-Williams and B. Schmidt at the Natural History Museum, UK. Preliminary analysis of NWA 12592 was performed by T. Hayden at The Open University.

Appendix A. Supplementary data

Supplementary data to this article can be found online at https://doi.org/10.1016/j.pss.2021.105287.

References

Ali, A., Jabeen, I., Gregory, D., Verish, R., Banerjee, N.R., 2016. New triple oxygen isotope data of bulk and separated fractions from SNC meteorites: evidence for mantle homogeneity of Mars. Meteoritics Planet Sci. 51 (5), 981–995. https://doi.org/10.1111/maps.12640.

Allen, C.C., Morris, R.V., McKay, D.S., 1994. Experimental reduction of lunar mare soil and volcanic glass. J. Geophys. Res.: Plan 99 (E11), 23173–23185. https://doi.org/10.1029/94JE02321.

Allen, C.C., Morris, R.V., McKay, D.S., 1996. Oxygen extraction from lunar soils and pyroclastic glass. J. Geophys. Res.: Plan 101 (E11), 26085–26095. https://doi.org/10.1029/96JE02726.

Altenberg, B.H., Franklin, H.A., Jones, C.H., 1993. Thermodynamics of lunar ilmenite reduction. In: 24th Lunar and Planetary Science Conference, pp. 27–28.

Barber, S.J., Wright, I.P., Abernethy, F.A.J., Anand, M., Dewar, K.R., Hodges, M., Landsberg, P., Leese, M.R., Morgan, G.H., Morse, A.D., Mortimer, J.I., Sargeant, H.M., Sheard, I., Sheridan, S., Verchovsky, A., Goesmann, F., Howe, C.J., Morse, T., Lillywhite, N., Trautner, R., 2018. ProSPA: analysis of lunar polar volatiles and ISRU demonstration on the Moon. In: 49th Lunar and Planetary Science Conference. #2172.

Britt, D.T., 1993. The spectral effects of subsolidus reduction of olivine and pyroxene. In: 24th Lunar and Planetary Science Conference, pp. 195–196.

Carpenter, J.D., Fisackerly, R., Houdou, B., 2016. Establishing lunar resource viability. Space Pol. 37, 52–57. https://doi.org/10.1016/j.spacepol.2016.07.002.

Carpenter, J.D., Hufenbach, B., Landgraf, S., de Mey, S., Borggraefe, A., Bergamasco, A., Sefton-Nash, E., Fisackerly, R., Houdou, B., de Rosa, D., Lefort, X., Trautner, R., Laurini, D., Schoonejans, P., Pastor, S., Hosseini, S., Braun, M., Parker, D., 2018. Lunar exploration plans in ESA. In: European Lunar Symposium.

Carrier III, W.D., Olhoeft, G.R., Mendell, W., 1991. Physical properties of the lunar surface. In: Heiken, G.H., Vaniman, D.T., French, B.M. (Eds.), Lunar Sourcebook. Cambridge University Press, pp. 475–594.

Carrier, W.D., 1973. Lunar soil grain size distribution. Moon 6 (3–4), 250–263. https://doi.org/10.1007/BF00562206.

Chambers, J.G., Taylor, L.A., Patchen, A., McKay, D.S., 1995. Quantitative mineralogical characterization of lunar high-Ti mare basalts and soils for oxygen production. J. Geophys. Res.: Plan 100 (E7), 14391–14401. https://doi.org/10.1029/95JE00503.

Cornish, L., Doyle, A., 1984. Use of ethanolamine thioglycollate in the conservation of pyritized fossils. Palaeontology 27 (Part 2), 421–424.

Gibson, M.A., Knudsen, C.W., Brueneman, D.J., Allen, C.C., Kanamori, H., McKay, D.S., 1994. Reduction of lunar basalt 70035: oxygen yield and reaction product analysis. J. Geophys. Res.: Plan 99 (E5), 10887–10897. https://doi.org/10.1029/94JE00787.

GmD Mineral Trade Company, 2020. Ilmenite powder. Accessed 9th March 2020. https://www.gmd-cologne.de/en/ilmenite_powder_en.html.

Graf, J.C., 1993. Lunar Soils Grain Size Catalog. NASA Reference Publication 1265. National Aeronautics and Space Administration, Lyndon B Johnson Space Center, Houston, Texas, US. https://www.lpi.usra.edu/lunar/surface/1LunarGrainFrontMatter.pdf.

Greenwood, R.C., Franchi, I.A., Gibson, J.M., Benedix, G.K., 2012. Oxygen isotope variation in primitive achondrites: the influence of primordial, asteroidal and terrestrial processes. Geochem. Cosmochim. Acta 94, 146–163. https://doi.org/10.1016/j.gca.2012.06.025.

Hadler, K., Martin, D.J.P., Carpenter, J.D., Cilliers, J.J., Morse, A.D., Starr, S., Rasera, J.N., Seweryn, K., Reiss, P., Meurisse, A., 2019. A universal framework for space resource utilisation (SRU). Planet. Space Sci. 104811. https://doi.org/10.1016/j.pss.2019.104811.

Hegde, U.G., Balasubramaniam, R., Gokoglu, S., Rogers, K., Reddington, M., Oryshchyn, L., 2011. Hydrogen reduction of lunar regolith simulants for oxygen production. 49th AIAA Aerospace Sciences Meeting Including the New Horizons Forum and Aerospace Exposition 608. https://doi.org/10.2514/6.2011-608.

Heiken, Grant H., 1975. Petrology of lunar soils. Rev. Geophys. 13 (4), 567–587. https://doi.org/10.1029/RG013i004p00567.

Keller, B.W., Clark, D.L., Kirkland, J.A., 2009. Field test results of the PILOT hydrogen reduction reactor. In: AIAA SPACE 2009 Conference & Exposition, p. 6475.

King, O., Warren, T., Bowles, N., Sefton-Nash, E., Fisackerly, R., Trautner, R., 2020. The Oxford 3D thermophysical model with application to PROSPECT/Luna 27 study landing sites. Planet. Space Sci. 182, 104790. https://doi.org/10.1016/j.pss.2019.104790.

Kleinhenz, J.E., Yuan, Z., Sacksteder, K., Caruso, J., 2009. Development of a reactor for the extraction of oxygen and volatiles from lunar regolith. In: 47th AIAA Aerospace Sciences Meeting Including the New Horizons Forum and Aerospace Exposition, p. 1203.

Kornuta, D., Abbud-Madrid, A., Atkinson, J., Barr, J., Barnhard, G., Bienhoff, D., Blair, B., Clark, V., Cyrus, J., DeWitt, B., others, 2019. Commercial lunar propellant architecture: a collaborative study of lunar propellant production. Reach. Out. 13, 100026. https://doi.org/10.1016/j.reach.2019.100026.

Lawrence, D.J., Feldman, W.C., Elphic, R.C., Little, R.C., Prettyman, T.H., Maurice, S., Lucey, P.G., Binder, A.B., 2002. Iron abundances on the lunar surface as measured by the Lunar Prospector gamma-ray and neutron spectrometers. J. Geophys. Res.: Plan 107. https://doi.org/10.1029/2001JE001530, 13-1-13-26–13.

Lee, K.A., Oryshchyn, L., Paz, A.J., Reddington, M., Simon, T.M., 2013. The ROxygen Project: outpost-scale lunar oxygen production system development at Johnson Space Center. J. Aero. Eng. 26 (1), 67–73. https://doi.org/10.1061/(ASCE)AS.1943-5525.0000230.

Lomax, B.A., Conti, M., Khan, N., Bennett, N.S., Ganin, A.Y., Symes, M.D., 2020. Proving the viability of an electrochemical process for the simultaneous extraction of oxygen and production of metal alloys from lunar regolith. Planet. Space Sci. 180, 104748. https://doi.org/10.1016/j.pss.2019.104748.

Lu, Y., Mantha, D., Reddy, R.G., 2010. Thermodynamic analysis on lunar soil reduced by hydrogen. Metall. Mater. Trans. B 41, 1321–1327. https://doi.org/10.1007/s11663-010-9411-3.

Manick, K., Gill, S.-J., Najorka, J., Duvet, L., 2018. Funadamental properties characterisation of lunar regolith simulants at the European Space Agency (ESA) sample analogue curaction facility. In: 49th Lunar and Planetary Science Conference, p. 1411.

Martins, Z., Hofmann, B.A., Gnos, E., Greenwood, R.C., Verchovsky, A., Franchi, I.A., Jull, A.J.T., Botta, O., Glavin, D.P., Dworkin, J.P., Ehrenfreund, P., 2007. Amino acid composition, petrology, geochemistry, ^{14}C terrestrial age and oxygen isotopes of the Shişr 033 CR chondrite. Meteoritics Planet Sci. 42 (9), 1581–1595. https://doi.org/10.1111/j.1945-5100.2007.tb00592.x.

Massieon, C.C., Cutler, A.H., Shadman, F., 1992. Reduction of iron-bearing lunar minerals for the production of oxygen. NASA Space Engineering Research Center for Utilization of Local Planetary Resources. N93-26676.

Massieon, C.C., Cutler, A.H., Shadman, F., 1993. Hydrogen reduction of iron-bearing silicates. Ind. Eng. Chem. Res. 32 (6), 1239–1244. https://doi.org/10.1021/ie00018a033.

McKay, D.S., Heiken, G.H., Basu, A., Blanford, G., Simon, S.B., Reedy, R., French, B.M., Papike, J.J., 1991a. The lunar regolith. In: Heiken, G.H., Vaniman, D.T., French, B.M. (Eds.), Lunar Sourcebook. Cambridge University Press, pp. 285–356.

McKay, D.S., Morris, R.V., Jurewicz, A.J., 1991b. Reduction of simulated lunar glass by carbon and hydrogen and its implications for lunar base oxygen production. In: 22nd Lunar and Planetary Science Conference, pp. 881–882.

Meteoritical Bulletin Database, 2019. Northwest Africa 12592. Accessed: 11th June 2019. https://www.lpi.usra.edu/meteor/metbull.php?code=69534.

Meyer, C., 2009. In: Meyer, Charles (Ed.), Lunar Sample Compendium, p. 10084. https://www.lpi.usra.edu/lunar/samples/atlas/compendium/10084.pdf.

Meyer, C., 2010. In: Meyer, Charles (Ed.), Lunar Sample Compendium, 60500 and 65510. https://curator.jsc.nasa.gov/lunar/lsc/60500.pdf.

Mortimer, J.I., 2016. *Investigating The Distribution And Source(s) of Lunar Volatiles* [Phd Thesis. The Open University. https://doi.org/10.21954/ou.ro.0000c4f3.

Retsch, 2004. The Basic Principles of Sieve Analysis. Accessed: 10th June 2019. https://www.retsch.com/downloads/application-reports/dl_details/1/file/53e4b553-2188-4f5f-b3ed-636500000000/.

Rickman, D.L., Lowers, H.A., 2012. *Particle Shape and Composition of NU-LHT-2m,* Report NASA/TM—2012–217458, National Aeronautics and Space Administration. Marshall Space Flight Center, Huntsville, Alabama, US. https://ntrs.nasa.gov/citations/20120011878.

Rickman, D.L., Young, C., Stoeser, D., Edmunson, J., 2014. Beneficiation of Stillwater Complex Rock for the Production of Lunar Simulants. Report NASA/TM-2014-217502, National Aeronautics and Space Administration. Marshall Space Flight Center, Huntsville, Alabama, US. https://ntrs.nasa.gov/citations/20140003187.

Sabat, K.C., Rajput, P., Paramguru, R.K., Bhoi, B., Mishra, B.K., 2014. Reduction of oxide minerals by hydrogen plasma: an overview. Plasma Chem. Plasma Process. 34, 1–23. https://doi.org/10.1007/s11090-013-9484-2.

Sanders, G.B., Larson, W.E., 2012. Progress made in lunar in situ resource utilization under NASA's exploration technology and development program. J. Aero. Eng. 26, 5–17. https://doi.org/10.1061/9780784412190.050.

Sargeant, H.M., Abernethy, F.A.J., Anand, M., Barber, S.J., Landsberg, P., Sheridan, S., Wright, I.P., Morse, A.D., 2020a. Feasibility studies for hydrogen reduction of ilmenite in a static system for use as an ISRU demonstration on the lunar surface. Planet. Space Sci. 180, 104759. https://doi.org/10.1016/j.pss.2019.104759.

Sargeant, H.M., Abernethy, F.A.J., Barber, S.J., Wright, I.P., Anand, M., Sheridan, S., Morse, A.D., 2020b. Hydrogen reduction of ilmenite: towards an in situ resource utilization demonstration on the surface of the Moon. Planet. Space Sci. 180, 104751. https://doi.org/10.1016/j.pss.2019.104751.

Schlüter, L., Cowley, A., 2020. Review of techniques for in-situ oxygen extraction on the Moon. Planet. Space Sci. 181, 104753. https://doi.org/10.1016/j.pss.2019.104753.

Sefton-Nash, E., Carpenter, J.D., Fisackerly, R., Trautner, R., Team, the E. S. A. L. E., group, the P. user, & team, the P. industrial, 2018. ESA's PROSPECT Package for Exploration of Lunar Resources: Investigation Domains. European Lunar Symposium.

Sefton-Nash, E., Fisackerly, R., Trautner, R., Barber, S.J., Reiss, P., Martin, D., Heather, D., Houdou, B., Team, the P. science, & Consortium, I, 2020. The ESA PROSPECT payload for Luna 27: development status. In: 51st Lunar and Planetary Science Conference, p. 2367.

Simon, S.B., Papike, J.J., Laul, J.C., 1982. The lunar regolith: comparative studies of the Apollo and Luna sites. Petrology of soils from Apollo 17, Luna 16, 20, and 24. In: 12th Lunar and Planetary Science Conference, pp. 371–388.

Spudis, P.D., Bussey, D.B.J., Baloga, S.M., Cahill, J.T.S., Glaze, L.S., Patterson, G.W., Raney, R.K., Thompson, T.W., Thomson, B.J., Ustinov, E.A., 2013. Evidence for water ice on the Moon: results for anomalous polar craters from the LRO Mini-RF imaging radar. J. Geophys. Res.: Plan 118, 2016–2029. https://doi.org/10.1002/jgre.20156.

Stoeser, D.B., Wilson, S., Rickman, D.L., 2010. *Design And Specifications For the Highland Regolith Prototype Simulants NU-LHT-1m and -2M*, Report NASA/TM—2010-216438. National Aeronautics and Space Administration, Marshall Space Flight Center, Huntsville, Alabama, US. http://citeseerx.ist.psu.edu/viewdoc/download?doi=10.1.1.185.1530&rep=rep1&type=pdf.

Sueyoshi, K., Watanabe, T., Nakano, Y., Kanamori, H., Aoki, S., Miyahara, A., Matsui, K., 2008. Reaction mechanism of various types of lunar soil simulants by hydrogen reduction. In: Earth & Space 2008: Engineering, Science, Construction, and Operations in Challenging Environments, pp. 1–8. https://doi.org/10.1061/40988(323)134.

Taylor, L.A., Carrier III, W.D., 1993. Oxygen production on the Moon: an overview and evaluation. In: Lewis, J.S., Matthews, M.S., Guerrieri, M.L. (Eds.), Resources of Near-Earth Space. University of Arizona Press, pp. 69–108.

Taylor, L.A., Jerde, E.A., McKay, D.S., Gibson, M.A., Knudsen, C.W., Kanamori, H., 1993. Production of O_2 on the Moon: a lab-top demonstration of ilmenite reduction with hydrogen. In: 24th Lunar and Planetary Science Conference, pp. 1411–1412.

Taylor, L.A., Liu, Y., 2010. Important considerations for lunar soil simulants. Earth and Space 2010: Engineering, Science, Construction, and Operations in Challenging Environments 106–118. https://doi.org/10.1061/41096(366)14.

The Lunar Sample Preliminary Science Team, 1972. Part A. A petrographic and chemical description of samples from the lunar highlands. In: Apollo 16 Preliminary Science Report. National Aeronautics and Space Administration, pp. 1–24.

Verchovsky, A.B., Anand, M., Barber, S.J., Sheridan, S., Morgan, G.H., 2020. A quantitative evolved gas analysis for extra-terrestrial samples. Planet. Space Sci. 181 https://doi.org/10.1016/j.pss.2019.104830.

Williams, R.J., 1985. Oxygen extraction from lunar materials: an experimental test of an ilmenite reduction process. Lunar Bases and Space Activities of the 21st Century 551.

Williams, R.J., McKay, D.S., Giles, D., Bunch, T.E., 1979. Mining and beneficiation of lunar ores. In: Billingham, J., Gilbreth, W., O'Leary, B. (Eds.), Space Resources and Space Settlements. National Aeronautics and Space Administration, pp. 188–275.

Zeng, X., He, C., Wilkinson, A., 2010. Geotechnical properties of NU-LHT-2M lunar highland simulant. J. Aero. Eng. 23 (4), 213–218. https://doi.org/10.1061/(ASCE)AS.1943-5525.0000026.

Zhao, Y., Shadman, F., 1993. Production of oxygen from lunar ilmenite. In: Lewis, J.S., Matthews, M.S., Guerrieri, M.L. (Eds.), Resources of Near-Earth Space. University of Arizona Press, pp. 149–178.